

# Reinforced Poly(ether sulfone) Materials by Blending with a Semiaromatic Liquid Crystalline Copolyester

M. García, J. I. Eguiazábal, J. Nazábal

*Departamento de Ciencia y Tecnología de Polímeros and Instituto de Materiales Poliméricos "Polymat," Facultad de Química, UPV-EHU, P.O. Box 1072, 20080 San Sebastián, Spain*

Received 28 January 2003; accepted 29 May 2003

**ABSTRACT:** Blends based on poly(ether sulfone) (PES) and a semiaromatic liquid crystalline copolyester (R5) were obtained by injection molding across the entire composition range. The blends showed two pure amorphous phases. The fibrillar structure of the skin led to enhancements in the stiffness. The break properties, however, decreased at low LCP contents, due to the expected lack of adhesion between the phases. The increase in the modulus at increasing LCP content led to improvements in tensile strength. The notch sensitivity of PES decreased after the addition of low LCP

levels, giving rise to enhancements of almost 600% in the notched impact strength. The unusually enhanced performance of the 20/80 blend, which has been seen previously in another thermoplastic/LCP blend, suggests that the dispersed PES phase in this blend may act as rubber particles do in rubber toughened thermoplastics. © 2003 Wiley Periodicals, Inc. *J Appl Polym Sci* 91: 52–59, 2004

**Key words:** blends; liquid-crystalline polymers (LCP); poly(ether sulfone); structure–property relations

## INTRODUCTION

The blends of thermoplastics and thermotropic liquid crystalline polymers (LCPs) are an important research field.<sup>1–3</sup> This is based on the ability of LCPs to orient in the flow direction, forming low viscosity *in situ* reinforced materials with greatly improved stiffness and tensile strength. Engineering polymers such as poly(butylene terephthalate), polyamides, polycarbonate, poly(ethylene terephthalate), and even polypropylene, have often been modified with LCPs; but the additional attractive properties of high-performance polymer matrices makes them natural candidates to be reinforced with LCPs.

Among high-performance thermoplastics, polysulfones have often been blended with LCPs. This is probably due to their widespread use in medical, food, and electrical and electronic applications. This is a consequence of their heat and solvent resistance, and hydrolytic stability, which will be retained after blending with LCPs.

The two most important polysulfones are polysulfone of bisphenol A (PSF) and poly(ether sulfone) (PES). Among the PSF/LCP blends, PSF/Vectra A (VA),<sup>4–7</sup> PSF/Rodrun 5000 (R5),<sup>8</sup> and PSF/aromatic polyester and copolyester LCP blends<sup>9,10</sup> have been

studied. These blends were processed mostly by extrusion,<sup>6–9</sup> and one by injection.<sup>4</sup> When the phase behavior or processability was studied, the blends were immiscible<sup>4,6–8</sup> and the LCP reduced the viscosity of the blends.<sup>4–6,10</sup> The injected PSF/VA blends<sup>4</sup> showed a fibrillar and well-developed layered LCP structure in the skin and a globular structure in the core. The stiffness was proportional to the composition, but only small increases in the tensile strength were observed.

With respect to PES/LCP blends, PES/VA,<sup>11–14</sup> PES/KU9231,<sup>15–20</sup> PES/Vectra B (VB),<sup>21</sup> PES/copolyester LCP,<sup>22</sup> PES/copolyesteramide LCP,<sup>22</sup> PES/R5,<sup>23</sup> and PES/aromatic copolyesters<sup>9,24</sup> blends were studied. Other articles on PES/LCP blends studied the transport properties of methanol in the blends<sup>25</sup> and measured the interfacial tension by different methods.<sup>12,26</sup> Both extruded<sup>9,18,19,21,22,24</sup> and injection-molded<sup>13–15,22</sup> PES-based blends were studied. The rest of the blends were processed by other methods. When the phase behavior or the interfacial adhesion was studied, both PES/VA<sup>13</sup> and PES/KU9231<sup>15–17</sup> blends were practically immiscible, although high interfacial adhesion was reported in PES/R5 blends.<sup>23</sup> The interfacial adhesion between the components of the blends is usually low.<sup>11,15,22</sup> The rheological studies indicated that the LCP decreased the viscosity, improving the processability of the blends in the case of both KU9231<sup>16,17,20</sup> and an aromatic copolyester.<sup>24</sup> The injected PES/KU9231,<sup>15</sup> PES/VA,<sup>13</sup> and other PES/LCP blends<sup>22</sup> showed skin-core morphology with higher fibrillation of the LCP in the skin. The addition of PES oligomers with reactive end groups as

Correspondence to: J. I. Eguiazábal (popegori@sq.ehu.es).

Contract grant sponsor: the University of the Basque Country; contract grant number: 9/UPV 00203.215-13540/2001.

a third component<sup>14</sup> has been used to improve the fibrillation of the LCP, which is difficult without high elongational flow. An extruded PES/copolyester LCP blend<sup>22</sup> showed longer fibrils in the core than in the skin. In the rest of the blends in which morphological studies were carried out,<sup>18,21,24</sup> the influence on fibrillation of different parameters, such as the draw ratio or the residence time in the die, was studied.

With respect to mechanical properties of injection-molded PES/LCP blends, the elastic modulus was additive in PES/KU9231 blends<sup>15</sup> and showed a slight negative deviation with respect to the rule of mixtures in PES/VA,<sup>13</sup> PES/copolyester, and PES/copolyester-amide blends.<sup>22</sup> However, and although the opposite has also been seen,<sup>22</sup> the strength increased less than the stiffness,<sup>15,19</sup> probably because of the immiscibility and the consequent low interfacial adhesion between the components. The flexural properties followed the behavior of the tensile properties,<sup>15,22</sup> and the impact strength of the blends decreased sharply.<sup>22</sup> The addition of a compatibilizer to PES/VA blends<sup>14</sup> had little effect on the flexural modulus, but flexural strength was clearly improved.

The LCPs used in most of these studies were VA<sup>11–14,25,26</sup> and KU9231.<sup>15–20</sup> Both LCPs are fully aromatic copolyesters. However, to our knowledge, there is only one study in which a commercial grade aromatic-aliphatic LCP has been used.<sup>23</sup> In this study the interfacial adhesion strength between PES and R5 was determined, but there was no discussion of the phase structure and mechanical properties of this blend.

The present work deals with blends based on a thermotropic copolyester (R5) and PES obtained by direct injection molding across the entire composition range. The structure of the *in situ* composites was characterized by means of thermal analysis (DSC and DMTA), scanning electron microscopy (SEM), and quantitative measurements of the orientation of the LCP by the orientation parameter. The effects of blending on the mechanical properties were studied by means of tensile and impact tests.

## EXPERIMENTAL

The polymers used in this work were commercial products. The PES was Ultrason E2010 (PES) from BASF, which has a viscosity number of 56 cm<sup>3</sup>/g. The LCP was Rodrun LC 5000 (R5) (Unitika). It is a semi-aromatic copolyester based on 80% poly(hydroxybenzoic acid) and 20% poly(ethylene terephthalate).

All blends were obtained by direct injection molding. After drying PES at 135°C for 15 h and R5 at 120°C for 12 h, injection molding of the blends across the entire composition range was carried out in a Battenfeld BA 230E reciprocating screw injection molding machine. The screw had a diameter of 18 mm, L/D of

17.8, compression ratio of 4, and helix angle of 17.8°. The barrel temperature was 330°C, and the mold temperature 30°C. An injection pressure of 1920 bar and an injection rate of 7.4 cm<sup>3</sup>/s were used.

The phase behavior of the blends was analyzed by differential scanning calorimetry (DSC) and dynamic-mechanical thermal analysis (DMTA). The DSC scans were carried out between 30 and 300°C in a Perkin-Elmer DSC-7 calorimeter at a heating rate of 20°C/min in a nitrogen atmosphere. Dynamic-mechanical tests were carried out in a TA Instruments DMA Q800 in flexural mode at a frequency of 1 Hz and a heating rate of 4°C/min from 30 to 270°C.

The polarized ATR spectra were carried out at a 45° angle of incidence using a Nicolet Magna-IR 560 spectrophotometer equipped with an ATR accessory (Spectra-Tech). The resolution was 8 cm<sup>-1</sup> and four measurements were carried out for each reported value. The calculation of the orientation parameter (*f*), which is related to the dichroic ratio, is explained elsewhere.<sup>27</sup> The average orientation is expressed as the orientation parameter.

The torques for kneading of the pure components were measured in a Brabender PLE 650 Plasticorder after drying. Kneading was carried out at 330°C and 50 rpm up to 7 min, when the torque steadied.

Tensile testing was carried out on 3.3 mm-thick tensile specimens (ASTM D-638, type IV) using an Instron 4301 tester at 23 ± 2°C with a crosshead speed of 10 mm/min. The Young's modulus (*E*), break stress ( $\sigma_b$ ) and ductility, measured as the break strain ( $\epsilon_b$ ), were obtained from the force–displacement curves. Notched Izod impact tests were carried out on a Ceast 6548/000 pendulum. The ASTM D-256 impact specimens used were 3.3 mm thick and their notches (depth = 2.54 mm and radius = 0.25 mm) were machined after injection molding. A minimum of eight specimens were tested for each reported value in both the tensile and impact tests.

The blend morphology was analyzed by scanning electron microscopy (SEM) (Hitachi S-2700) after gold coating (Fine Coat Jeol Ion Sputter JFC-1100). The accelerating voltage was 15 kV. The skin thickness was measured on low-magnification SEM photomicrographs. A minimum of six measurements were done and a minimum of two specimens were used, for each reported skin thickness value.

## RESULTS

### Phase behavior

When the blends and the pure components were observed by DSC, in agreement with previous studies,<sup>8,28</sup> the  $T_g$  of the neat R5 appeared at approximately 75°C, and its melting endotherm was composed of various small peaks between 280 and 290°C. However,

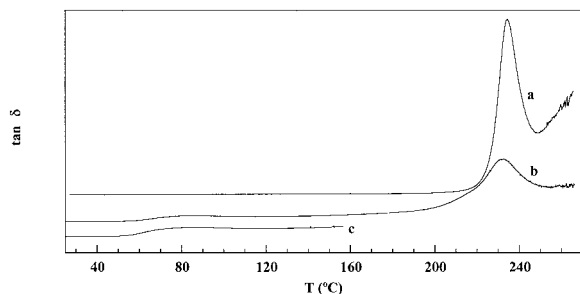


**Figure 1** DMTA plots of pure PES (a), R5 (c), and the 60/40 blend (b).

neither the  $T_g$  nor the  $T_m$  of R5 were detectable in the blends, probably due to the small heat capacity increase of its  $T_g$  and its low melting heat. Thus, the phase behavior of the blends was studied by DMTA. Figure 1 shows the  $\tan \delta$  curve of the 60/40 PES/R5 blend, as an example, and those of the neat components. The rest of the blends gave similar results. As can be seen, the  $\tan \delta$  peaks corresponding to both R5 (86°C) and PES (233°C), appeared at the same temperatures both in the blends and in the pure components. As in the case of both polysulfone and polyarylsulfone with R5,<sup>8</sup> this indicated full immiscibility and the presence of two pure amorphous phases in the blends.

### Morphology

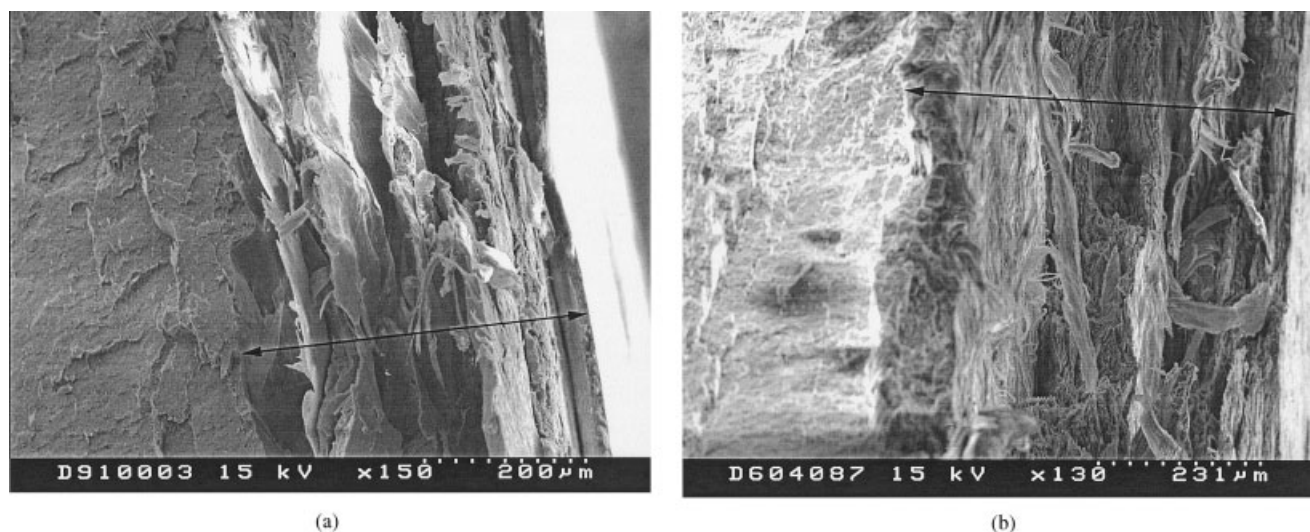
As usual in *in situ* composites,<sup>3,13</sup> the SEM of cryogenically fractured surfaces of the tensile specimens showed both skin and core zones at low R5 contents. The skin was clearly defined, with much higher fibrillation of the LCP than in the core. The higher fibrillation of the skin is a consequence of its higher shear

**TABLE I**  
Mean Skin Thickness of the Blends vs R5 Content

| % R5 | Skin thickness ( $\mu\text{m}$ ) |
|------|----------------------------------|
| 10   | 455                              |
| 20   | 510                              |
| 30   | 570                              |
| 40   | 625                              |

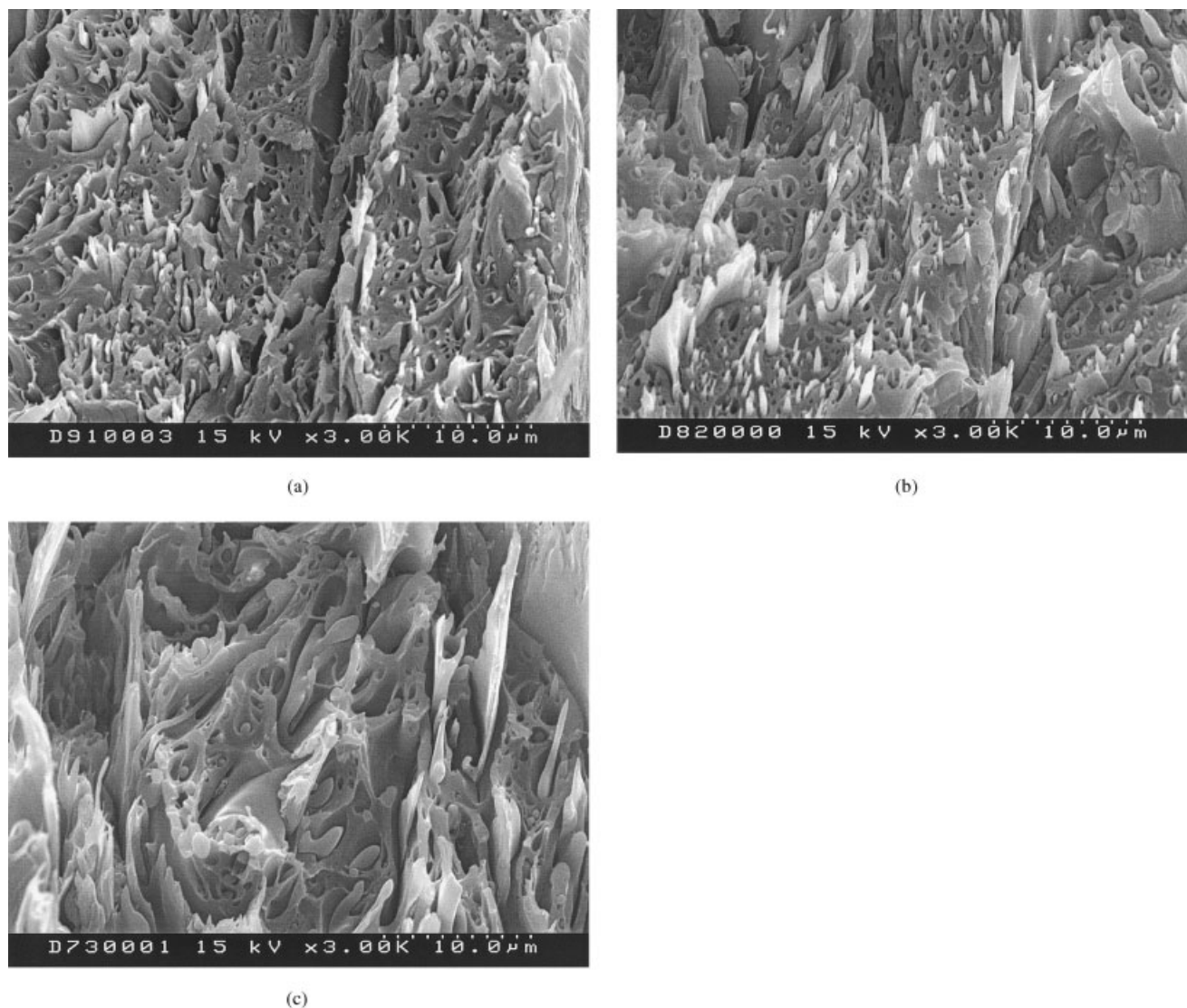
flow. Other injected blends, such as PSF/VA<sup>4</sup> or PES/VA<sup>14</sup> showed similar morphologies. In other injected PES-based blends,<sup>13,22</sup> there were some morphological differences, especially in the core. The morphology was not reported in ref. 15. The thickness of the skin has an important effect on the mechanical properties as a consequence of its morphology. Consequently, it was measured at low magnification, as indicated in Figure 2, and the results are collected in Table I as a function of the LCP content.

Figure 3(a), (b), and (c) show the morphology of the skin of the blends with 10, 20, and 30% R5. As can be seen, the R5 particles are elongated. Thus, in the skin of the 90/10 blend of Figure 3(a), thin LCP fibrils appeared embedded in the PES matrix. In the skin of the 80/20 blend of Figure 3(b), the fibers were longer and thicker and large structures started to appear. This took place in PSF/VA blends<sup>4</sup> at 30% VA. The morphology of the 70/30 blend of Figure 3(c) was rather complex; besides fibrillar zones, both bundles of highly oriented LCP fibers and some large LCP structures were present. The 60/40 blend showed a similar morphology in which very few fibers were observed. Other PES/LCP blends<sup>13,22</sup> also showed sheets and large structures in the skin. In the rest of the blends no skin could be differentiated in the spec-



**Figure 2** Low magnification SEM photomicrographs of PES/R5 blends at R5 contents of (a) 10% and (b) 30%. The arrows indicate the thickness of the skin.





**Figure 3** SEM photomicrographs of the skin section of cryogenically fractured tensile specimens of PES/R5 blends at R5 contents of (a) 10%, (b) 20%, and (c) 30%.

imens. Quantitative measurements of the orientation will be discussed later. The voids that surrounded the particles suggested poor interfacial adhesion, which is typical of LCP blends.

Figure 4 shows the morphology of the core of the PES/R5 blends. In the case of the 90/10 blend, the LCP phase appeared as small spherical particles (1.0–4.0  $\mu\text{m}$ ) and the dispersed phase size distribution was narrow and rather homogeneous. In the 80/20 PES/R5 blend of Figure 4(a), both a spherical morphology (60% of the core), similar to that of the 90/10 blend, and large planar shape and minor R5 domains such as those of Figure 4(b) were observed. In PES/VA blends<sup>14</sup> the heterogeneity of the blends, mainly in the core, was also high. The 70/30 blend and also the 60/40 blend [Fig. 4(b)] showed both a spherical morphology, and LCP domains slightly larger

than those of Figure 4(a). In the center of the core, probably because of viscosity effects, the LCP domains were interconnected, revealing the proximity of phase inversion. The core of both PSF/VA<sup>4</sup> and PES/VA<sup>14</sup> blends at high LCP contents showed large irregular domains and big particles. In other injected PES/LCP blends,<sup>13,22</sup> however, some thin fibrils with aspect ratios that decreased with increasing LCP content were present in the core. In the blends of this study, the LCP content appears to be less than the overall composition, suggesting that R5 migrates to the high shear level skin.

The determination of the composition where phase inversion takes place is difficult when the viscosities of the two components of the blends are very different, as in this case. Thus, when the  $\Phi_{21} = 1/(1 + \lambda)$  expression<sup>29</sup> was used, where  $\lambda = \eta_d/\eta_m$  and  $\eta_d$  and  $\eta_m$  are

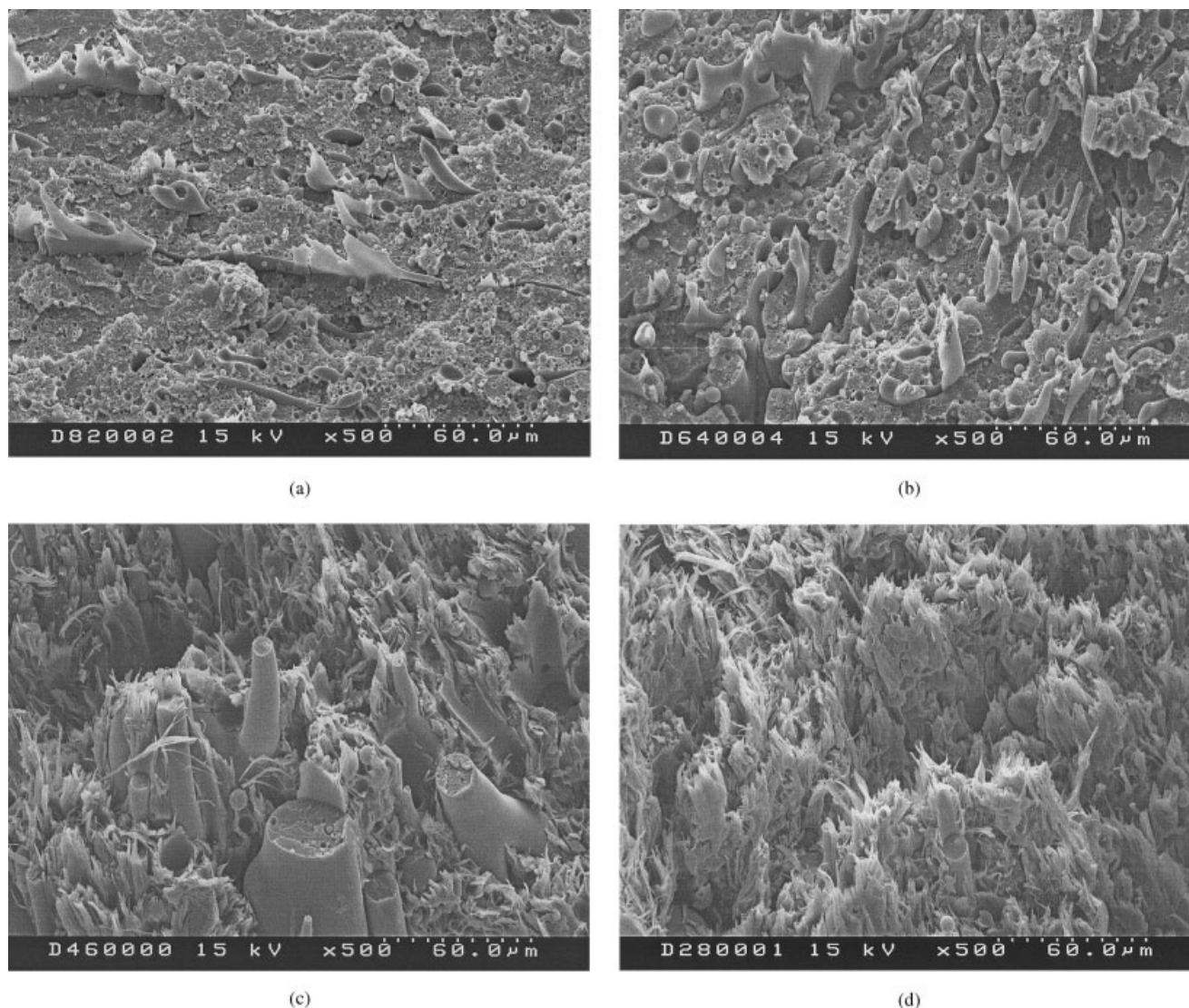


**Figure 4** SEM photomicrographs of the core section of cryogenically fractured tensile specimens of PES/R5 blends at R5 contents of (a) 20%, (b) 40%, (c) 60%, and (d) 80%.

the viscosities of the dispersed phase and the matrix, respectively, with  $\lambda$  calculated from the values for the torque of kneading, the obtained result (1% R5) was unrealistic. When a more complex expression such as  $\lambda = [(\phi_m - \phi_{2l}) / (\phi_m - \phi_{1l})]^{[\eta] \phi_m}$  was applied,<sup>29</sup> where  $\phi_m$  is the maximum packing volume fraction,  $[\eta]$  the intrinsic viscosity, and  $\phi_{2l}$ ,  $\phi_{1l}$  correspond to the phase inversion composition, the obtained intrinsic viscosity was slightly out of the expected range. The phase inversion composition (16% R5) disagreed also with the observed morphology, because R5 was the dispersed phase in the 60/40 blend.

In the blends with 60% R5 [Fig. 4(c)], PES appeared as the dispersed phase in a highly oriented LCP structure. The morphology of the 20/80 blend [Fig. 4(d)] was the highly fibrillated structure typical in LCPs, with some PES islets finer than in Figure 4(c).

### Mechanical properties

The Young's moduli of the PES/R5 blends are shown in Figure 5 as a function of the R5 content. As can be seen, the modulus increased continuously with increasing R5 content, and it was close to the reference of the single rule of mixtures. This rather linear behavior of the modulus of elasticity is typical of immiscible and uncompatibilized blends,<sup>4,30</sup> and has been previously seen in other PES/LCP blends.<sup>19,22</sup> However, modulus values below those of the single (parallel constant strain) rule of mixtures were seen in PES/VA blends,<sup>13</sup> and in the case of flexural modulus of PES/VA blends,<sup>14</sup> in which the importance of the highly oriented skin is larger, helping high flexural modulus values. Considering the reason for these two different modulus behaviors, moduli close to linearity

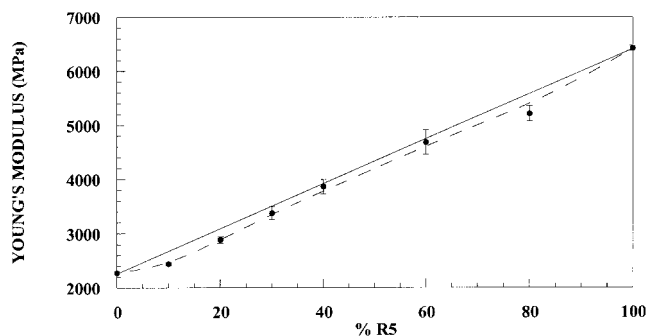


Figure 5 Young's modulus of the blends vs R5 content.

should be due to larger orientation and fibrillation of the LCP fibers in the blends. An attempt was made to find out whether any parameter that influences orientation, such as the viscosity ratio, the thickness of the specimen, the core/skin thickness ratio, or the geometry of the nozzle, was the main factor responsible for the different behaviors. This was made comparing, where available, these parameters in the case of linear modulus behavior<sup>4,19,22</sup> with the same parameters in the case of performance below linearity.<sup>13,14</sup> However, no direct relation of fibrillation to any of the parameters mentioned was found. This was probably because most of those parameters influenced fibrillation as a whole. Finally, the mostly linear behavior of the modulus of elasticity of this study, which is often seen in thermoplastic/LCP blends, indicates that interfacial adhesion is not necessary for the properties of the dispersed phase to be transmitted to the matrix at the low strain at which the modulus is measured.

With respect to the morphological characteristics that influence the modulus of elasticity, the orientation level of the LCP in the skin and the skin thickness are the main parameters. For this reason, the orientation was measured by the orientation parameter and the data are collected in Table II. The orientation parameter was highest at low LCP contents and decreased with increasing LCP content. This agrees with the observation of thin LCP fibers at low LCP contents, which should reinforce the matrix more than the com-

TABLE II  
Orientation Parameter of R5 in the Skin vs R5 Content

| %R5 | f           |
|-----|-------------|
| 10  | 0.30 ± 0.04 |
| 20  | 0.28 ± 0.02 |
| 30  | 0.25 ± 0.02 |
| 40  | 0.22 ± 0.02 |
| 60  | 0.21 ± 0.02 |
| 80  | 0.21 ± 0.02 |
| 100 | 0.22 ± 0.02 |

TABLE III  
Ductility of the Blends vs R5 Content

| % R5 | $\epsilon_b$ (%) |
|------|------------------|
| 0    | 74 ± 8           |
| 10   | 4.0 ± 0.2        |
| 20   | 3.4 ± 0.2        |
| 30   | 3.4 ± 0.2        |
| 40   | 3.2 ± 0.1        |
| 60   | 2.8 ± 0.2        |
| 80   | 3.0 ± 0.1        |
| 100  | 2.6 ± 0.2        |

plex structure of higher compositions did. This higher performing morphology should have led to a higher slope of the modulus vs composition curve than that of Figure 5. However, as was seen in Table I, at low R5 contents the thickness of the skin was lowest. This counteracts its higher fibrillation and must be the reason for the rather linear behavior of the modulus of Figure 5.

Table III shows the ductility of the blends measured as the elongation at break. The addition of R5 to the blends, as usual in *in situ* composites,<sup>30,31</sup> and due to the brittle nature of the LCPs, led to a strong decrease in ductility. The decrease in ductility of the blends at increasing R5 content agrees with the coarsening morphology of the R5-poor blends at increasing R5 content.

The tensile strength of the blends is plotted in Figure 6 as a function of the R5 content. With the exception of the 20/80 composition, the deviation below linearity was clear. This is a consequence of the ductility drop in the blends, as the other factor that influences tensile strength in these brittle materials, that is, the modulus of elasticity, shows a basically linear behavior. The unexpected high tensile strength of the 20/80 composition is due to its higher ductility compared with both that of pure R5 and the 40/60 blend.

The similarity in the tensile strength between the 20/80 blend and the pure R5 is an interesting result, taking into account the higher price of R5. It is an unexpected result, but it is not the first time such

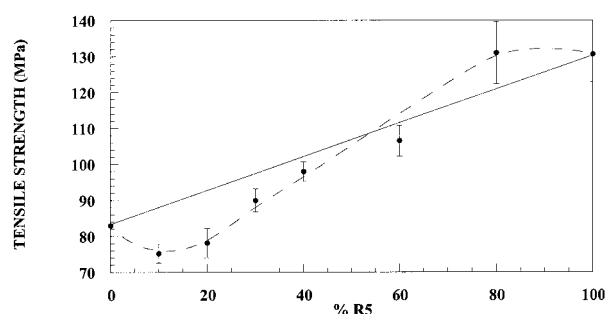
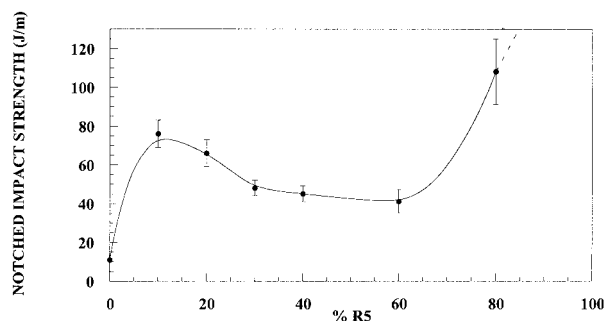


Figure 6 Tensile strength of the blends vs R5 content.





**Figure 7** Notched Izod impact strength of the blends vs R5 content.

behavior has been observed. In fact, the tensile strength of amorphous polyamide/VB blends was even higher than that of pure VB at large VB contents.<sup>32</sup> Moreover, an additional unpublished study on the impact strength of amorphous polyamide/VB blends, showed that the impact strength of the 20/80 blend was much larger than that of pure VB, as the blend did not break upon impact testing whereas the pure VB did. Both the large modulus difference between the two components of these thermoplastic/LCP blends, and the rigid nature of the LCPs, are similar to phenomena found in rubber toughened thermoplastic blends. In the latter, the dispersed soft particles act as stress concentrators modifying the fracture behavior of the pure matrix and clearly leading to both larger impact strength and ductility. This is a tentative explanation for such behavior, that is, that PES could act as a toughening agent. Whether this behavior is found in other thermoplastic/LCP blends, and the reasons for it, are the following tasks in this research area.

The notched impact strength of the blends is plotted against R5 content in Figure 7. Pure R5 did not break. As can be seen, the addition of only 10% R5 led to a dramatic increase in the impact strength of the pure PES matrix of almost 600%. This is attributed to the reduction of the high notch sensitivity of PES due to the R5 presence. This is supported by the fact that the unnotched impact strength of PES decreased on R5 addition, as did ductility, while the opposite took place in notched specimens. The impact values at high R5 contents cannot be properly evaluated, because they cannot be compared with that of pure R5 under the present test conditions, as R5 did not break. However, the 20/80 composition showed the highest notched impact strength. It cannot be ruled out that blends with smaller PES content, and as a consequence, smaller dispersed particle size, and even smaller distance between particles, led to larger impact strength values comparable to those of pure R5.

## CONCLUSIONS

The PES/R5 blends were composed of two pure amorphous phases. Both SEM micrographs and orientation, measured as the orientation parameter, indicated that fibrillation of R5 was higher at low LCP contents where skin thickness was thinner. The thin fibrils of the skin at low R5 contents became thicker and formed large LCP structures at increasing LCP content. The morphology of the core was mainly spherical at low LCP contents; at higher LCP contents, some large planar-like domains were also present. The interfacial adhesion was poor.

The Young's modulus increased with the R5 content, and was close to that predicted by the linear rule of mixtures, whatever the composition. The tensile strength was below linearity, mainly as a consequence of the ductility drop in the blends. This was with the exception of the 20/80 composition, which exhibited a tensile strength similar to that of the pure R5. The low notched impact strength of PES increased dramatically after the addition of 10% LCP, thus reducing the large notch sensitivity of PES.

Both the unusually high tensile strength of the 20/80 composition, and the previously observed exceptional tensile and impact strength performance of another thermoplastic/LCP blend, suggest that a small dispersed thermoplastic phase in a LCP matrix may modify the fracture behavior of LCPs. This modification of the fracture behavior may be similar to that which rubber induces in low impact strength thermoplastics, leading to rubber-toughened blends.

The authors would like to express their gratitude to BASF for providing PES. M. García acknowledges the Spanish "Ministerio de Educación y Ciencia" for the award of a grant.

## References

1. La Mantia, F. P. *Thermotropic Liquid Crystal Polymer Blends*; Technomic Publishing Inc.: Lancaster, PA, 1993.
2. Acierno D.; La Mantia, F. P. *Processing and Properties of Liquid Crystalline Polymers and LCP Based Blends*; ChemTec Publishing: Toronto, 1993.
3. Acierno, D.; Collyer, A. A. *Rheology and Processing of Liquid Crystal Polymers*; Chapman & Hall: London, 1996.
4. Golovoy, A.; Kozlowsky, M.; Narkis, M. *Polym Eng Sci* 1992, 32, 854.
5. La Mantia, F. P.; Paci, M.; Magagnini, P. L. *Rheol Acta* 1997, 36, 152.
6. Magagnini, P. L.; Paci, M.; La Mantia, F. P.; Surkova, I. N.; Vasnev, V. A. *J Appl Polym Sci* 1995, 55, 461.
7. Hong, S. M.; Kim, B. C.; Kim, K. U.; Chung, I. J. *Polym J* 1991, 23, 1347.
8. Jung, H. C.; Lee, H. S.; Chung, Y. S.; Kim, S. B.; Kim, W. N. *Polym Bull* 1998, 41, 387.
9. He, J.; Bu, W.; Zhang, H. *Polym Eng Sci* 1995, 35, 1695.
10. Skovby, M. H. B.; Kops, J.; Weiss, R. A. *Polym Eng Sci* 1991, 31, 954.

11. Machiels, A. G. C.; Van Dam, J.; Posthuma de Boer, A.; Norder, B. *Polym Eng Sci* 1997, 37, 1512.
12. Machiels, A. G. C.; Van Dam, J.; Posthuma de Boer, A. *Polym Eng Sci* 1998, 38, 1536.
13. Engberg, K.; Strömberg, O.; Martinsson, J.; Gedde, U. W. *Polym Eng Sci* 1994, 34, 1336.
14. Yazaki, F.; Kohara, A.; Yosomiya, R. *Polym Eng Sci* 1994, 34, 1129.
15. Shi, F.; Yi, X. S. *Int J Polym Mater* 1995, 28, 227.
16. Shi, F.; Yi, X. S. *Int J Polym Mater* 1994, 25, 243.
17. Yi, X. S.; Zhao, G.; Shi, F. *Polym Int* 1996, 39, 11.
18. Wang, H.; Yi, X. S.; Hinrichsen, G. *Polym J* 1997, 29, 881.
19. Shi, F. *Polym Plast Tech Eng* 1994, 33, 445.
20. Yi, X. S.; Zhao, G. *J Appl Polym Sci* 1996, 61, 1655.
21. Wiff, D. R.; Weinert, R. J. *Polymer* 1998, 39, 5069.
22. Kiss, G. *Polym Eng Sci* 1987, 27, 410.
23. Cho, K.; Kong, T.; Lee, D. *Polym J* 1997, 29, 904.
24. He, J.; Bu, W. *Polymer* 1994, 35, 5061.
25. Wiberg, G.; Hedenqvist, M. S.; Boyd, R. H.; Gedde, U. W. *Polym Eng Sci* 1998, 38, 1640.
26. James, S. G.; Donald, A. M.; Miles, I. S.; Mallagh, L.; MacDonald, W. A. *J Polym Sci Polym Phys* 1993, 31, 221.
27. García, M.; Eguiazábal, J. I.; Nazábal, J. *J Polym Sci Polym Phys* 2003, 41, 1022.
28. Vallejo, F. J.; Eguiazábal, J. I.; Nazábal, J. *Polym J* 2001, 33, 128.
29. Utracki, L. A. *J Rheol* 1991, 35, 1615.
30. Bastida, S.; Eguiazábal, J. I.; Nazábal, J. *Eur Polym J* 1999, 35, 1661.
31. Vallejo, F. J.; Eguiazábal, J. I.; Nazábal, J. *Polym Eng Sci* 1999, 39, 1726.
32. García, M.; Eguiazábal, J. I.; Nazábal, J. *Polym Eng Sci* 2002, 42, 413.